Available online at www.sciencedirect.com
SCIENCE DIRECT®
Earth and Planetary Science Letters 237 (2005) 167–174
EPSL
www.elsevier.com/locate/epsl

The in situ pH of hydrothermal fluids at mid-ocean ridges

Kang Ding[a,*], William E. Seyfried Jr.[a], Zhong Zhang[a], Margaret K. Tivey[b], Karen L. Von Damm[c], Albert M. Bradley[b]

[a]*Department of Geology and Geophysics, University of Minnesota, Minneapolis, MN 55455, USA*
[b]*Woods Hole Oceanographic Institution, Woods Hole, MA 02543, USA*
[c]*Complex System Research Center, University of New Hampshire, 39 College Rd. Durham, NH 03824-3525, USA*

Received 9 August 2004; received in revised form 22 March 2005; accepted 25 April 2005
Available online 21 July 2005
Editor: E. Boyle

Abstract

Here we report the first in situ pH of hydrothermal vent fluids at mid-ocean ridges. Measurements were made during dives with DSV Alvin to the Main Endeavour Field (Juan de Fuca Ridge) and the East Pacific Rise at 21°N, and 9°–10°N using solid-state electrochemical sensors. Vent fluid temperature and pressure ranged from 180 to 384 °C and 220 to 250 bar, respectively. $pH_{(in\ situ)}$ of the highest temperature vent fluid is only slightly acidic (5.1–5.4), although sharply lower values occur at the seawater/vent-fluid interface. Knowledge of $pH_{(in\ situ)}$ is essential for unravelling the complex geochemical and biogeochemical processes controlling the evolution of seafloor hydrothermal systems.
© 2005 Elsevier B.V. All rights reserved.

Keywords: hydrothermal fluid; in situ pH; mid-ocean ridges

1. Introduction and background

Since the discovery of deep-sea hydrothermal vents more than 25 yr ago, numerous efforts have been made to determine the pH of the hot venting fluid [1–8]. Owing to the extreme physical and chemical conditions at seafloor vents, however, direct pH measurement has not been possible, encouraging development of indirect approaches [3,5,6]. The challenge of determining pH of a chemically complex fluid at elevated temperatures and pressures ($pH_{(in\ situ)}$) involves the need to explicitly account for temperature and pressure dependent changes in the distribution of aqueous species. Dissociation of H^+ and OH^--bearing aqueous complexes and ion pairs in response to cooling of a hydrothermal fluid to ambient seafloor conditions results in pH change, as follows:

$$mH^+_{25\,^\circ C} = \sum mHX^\circ_{T,P} + mH^+_{T,P} - \sum mYOH^\circ_{T,P} \quad (1)$$

where HX° and YOH° represent idealized acids and bases, respectively — the stability of which are

* Corresponding author. Tel.: +1 612 626 1860; fax: +1 612 625 3819.
E-mail address: mlcd@umn.edu (K. Ding).

0012-821X/$ - see front matter © 2005 Elsevier B.V. All rights reserved.
doi:10.1016/j.epsl.2005.04.041

explicit functions of temperature, pressure and fluid composition. Thus, the amount of free H^+ in the quenched fluid ($mH^+_{25\ ^\circ C}$) is clearly not the same as that at high temperature and pressure ($mH^+_{T,P}$). This is especially true for hydrothermal fluids near the critical point of seawater (408 °C) [9,10] where H^+-bearing aqueous complexes are particularly stable, but which can be rendered unstable with slight chemical and physical change. In addition to temperature and pressure dependent changes in homogeneous equilibria, cooling induced precipitation of metal sulphides and oxides from venting fluid, oxidation to metal oxyhydroxides and disproportionation of sulphur gases in plumes also affect pH. In spite of these difficulties, knowledge of vent fluid pH is sufficiently important to so many geochemical and biogeochemical processes at and below the seafloor that efforts to develop successful direct measurement strategies at elevated temperatures and pressures are well justified.

2. Methods and material

2.1. Sensor design and construction

Recent advances in material science, sensor technology, and experimental and theoretical geochemistry, have permitted development of pH sensors for use in seafloor hydrothermal systems. One such sensor makes use of YSZ (yittria-stabilized zirconia) ceramic, which has been used with success in laboratory studies to determine pH of aqueous fluids at high temperatures [11,12]. The solid-state design and its specific and response to a^+_H make the YSZ-based sensor well suited for seafloor applications. In its initial seafloor deployment, however, the YSZ-sensor was configured in such a way that pH was not explicitly determined, but rather pH response served as a reference permitting measurement of dissolved H_2 and H_2S [13]. In the present study, this configuration was changed in that the YSZ-sensor was combined with a Ag–AgCl reference electrode allowing $pH_{(in\ situ)}$ to be explicitly determined.

$$Ag|AgCl|Cl^-, H^+, H_2O|YSZ|Hg|HgO \qquad (2)$$

The cell potential ($\Delta E(V)_{TP}$) for Eq. (2) can be given as

$$\Delta E(V)_{TP} = \Delta E(V)^\circ_{TP} - \frac{2.303RT}{F} \times \left[\log a(Cl^-) - \frac{1}{2}\log a(H_2O) - pH_{(in\ situ)}\right] \qquad (3)$$

Change in fluid pH will result a substantial change in sensor's emf signal. For instance, at 375 °C, one pH unit variation will result a change of 0.129 V for $\Delta E(V)_{TP}$, which is given by Nernstian slope in Eq. (3). Thus, $pH_{(in\ situ)}$ of a fluid at an elevated temperature and pressure, can be determined through the measurement ($\Delta E(V)_{TP}$) [12]:

$$pH_{(in\ situ)} = \frac{F}{2.303RT}\left[\Delta E(V)_{T,P} - \Delta E(V)^\circ_{TP}\right] + \left[\log a(Cl^-) - \frac{1}{2}\log a(H_2O)\right] \qquad (4)$$

where $\Delta E(V)^\circ_{TP}$ is the standard cell potential at appropriate temperatures and pressures as determined from standard state potentials of $E_{Ag/AgCl}(V)^\circ_{TP}$ and $E_{Hg/HgO}(V)^\circ_{TP}$; R is the gas constant; F is the Faraday constant; and, $a(Cl^-)$ and $a(H_2O)$ are the activities of dissolved chloride and H_2O, respectively. Activity of dissolved chloride is determined from the measured total chloride concentration taking explicit account of distribution of aqueous species calculations using appropriate thermodynamic data [14–24].

Titanium metal was selected for construction of the sensor housing. In general, the sensor can be defined in terms of three subunits: (1) electrode assembly; (2) transition unit; and, (3) electronics package. The electrode assembly is located at the tip of the sensor and housed in a titanium casing. The Ti-casing was designed to enhance the flow of fluid passing the electrodes, while at the same time protecting the electrodes from potential impact with rock or chimney structures. The outer diameter of the Ti-case holding the electrode assembly is 2.5 cm. A distance less than 0.5 cm separates all electrodes, including the Ti-sheathed J or E type thermocouple [see Fig. 4 in 13]. Moreover, the response region of the electrodes is limited to 0.6 cm from the tip, which allows unusually

precise control of chemical (pH) measurements in specific thermal regimes in vent fluid systems. The electrode assembly is pressure sealed using a modified Conax fitting and associated Teflon sealant (Conax Buffalo, NY), effectively precluding penetration of seawater or vent fluid into the other subunits of the sensor.

The pressure housings containing the transition unit and electronics package are constructed of titanium alloy (6Al4V) for mechanical strength. The titanium alloy housing prevents seawater access to the electrical contacts leading to the electrode assembly or the electronics package, where signal processing is carried out. Moreover, the Ti-alloy provides an effective shield for the high impedance and low voltage signals generated from the sensors against possible signal interference from other electrical operations involving the submersible. Viton and Teflon O-rings are used in these two subunits as pressure sealants. The electronics package subunit is contained in a cylindrical Ti-housing (20.32 cm (*l*), 7.30 cm (o.d.), and 2.70 cm (wall thickness)). This subunit contains all the requisite electronic components and batteries for signal processing and transmission. The total length and weight of an assembled sensor unit is approximately 1 m and 5 kg (in air), respectively. For more easily sampling fluids issuing from chimney structures and flange pools using the manipulator on *Alvin*, the front end of the sensor unit is tilted at a 30° angle (Fig. 1).

2.2. Data communications

The electronics package involves three major subsystems: an electrometer for processing high impedance DC voltage from the pH sensor; an analogue to digital converter to digitise the electrometer outputs and the thermocouple voltages; and a microcomputer to scan the inputs and communicate with the submersible. Data transfer is accomplished by inductively coupled link (ICL) [25]. Seven AA cells power the system. The power consumption is only 23 mA and the unit will shut down if not called upon within 1 min. In "sleep" mode the unit requires as little as one μA of power. In general, the ICL interface allows non-contact communication between the submersible and the sensors via a pulsed magnetic field from a simple coil of wire at any baud rate up to 9600. The ICL system uses two or more magnetic coils (links) with associated electrical interface, which serve as modems. Two types of modems exist, one that interfaces

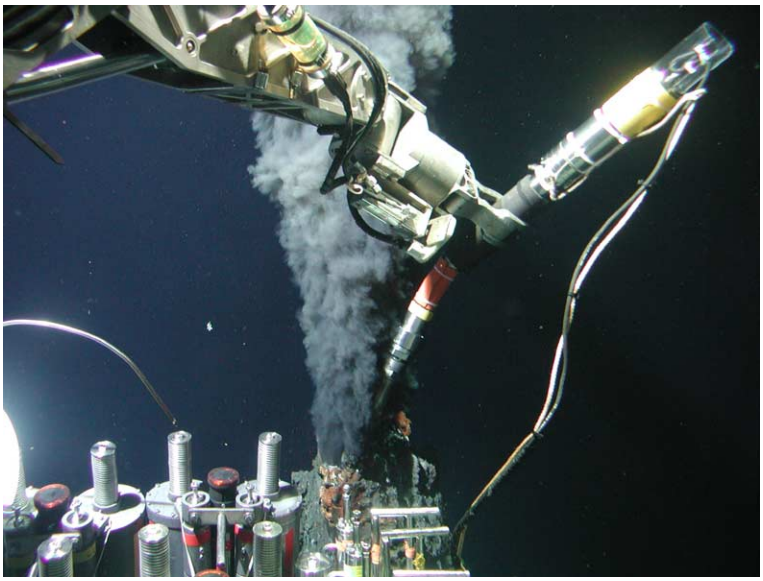

Fig. 1. Sensor unit being positioned by the manipulator arm of DSV Alvin beneath the orifice of the chimney structure at SW vent (21°N EPR) during dive 3749 to obtain high temperature $pH_{(in\ situ)}$ data. The illustration also reveals the relative distance between the sensor head immersed in the vent fluid and the electronics package (rear of sensor). The yellow region at the base of the electronics package is approximately 15 cm. The data from the sensor were transmitted inductively through an ICL cable connection into the submersible in real time.

to a computer inside the submersible via true RS-232 communication, and another built into the sensor's electronics package. The modem internal to the sensor contains a 5 V CMOS interface to minimize power consumption. The modems operate using an unregulated power supply providing between 8 and 15 V. Separation between the magnetic loops can be as great as 10 cm at 12 V, although actual operations are conducted at distances always considerably less than this. Use of inductive loops provides total electrical isolation between the sensor and the submersible. Since it is possible to deploy more than one inductive link, simultaneous data transmission from multiple chemical sensors is possible simply by uniquely addressing each unit. WinWedge (TALtech, Philadelphia, PA) software is used to acquire and store real-time data into a computer in the submersible for data processing.

2.3. Measurement

Measurements of fluid chemistry were made in hydrothermal fluids at a wide range of temperatures to determine $pH_{(in\ situ)}$ of the hydrothermal end-member, but also to constrain pH response to the effects of seawater mixing, cooling and mineralization [26–28]. In situ sensor data are recorded at the rate of 3~5 s per reading. In addition to the obvious advantage of visual observation, simultaneous temperature and pH measurements in real time enhance the success of sensor applications in the challenging and dynamic vent environment. The sensor performance was verified through laboratory experiments at similar T and P conditions. Calibration of the thermocouple was independently conducted through Entherm (Bloomington, MN) following ASTME230 standard (± 1.7 °C for type-E, ± 2.2 °C for type-J). For the field measurements, pH values are determined from sensor and temperature data after readings achieve steady state values, which are indicated by variability of less than ± 0.005 V and ± 3 °C for $\Delta E(V)_{TP}{}^{\circ}$ and T, respectively. Thus, for pH data, the inherent uncertainties from the sensor are on the order of ± 0.02 pH units. As indicated earlier, however, dissolved Cl concentration is also a necessary consideration. Uncertainties on this parameter will contribute to errors in pH data, although the form of the Nernst equation mitigates the magnitude of this. For instance, even with an uncertainty of ± 100 mM in total dissolved Cl concentration, the corresponding variation to pH value would be $\sim \pm 0.05$. Owing to the more serious uncertainties associated with the thermodynamic database used to calculate a(Cl-) , overall errors in reported pH values can be as high as ± 0.1 units.

3. Results and discussion

Ten vents on three different ridge segments were visited during three cruises over a three-year interval. Efforts were initially focused on high temperature vent fluids. Thus, pH measurements were made at the Main Endeavour Field (Juan de Fuca Ridge) and at 21°N and 9°–10°N (East Pacific Rise). The seafloor depth in these areas is approximately 2200 and 2500 m, respectively [26,27]. Sensor measurements were made using two distinct deployment strategies. The first involved pH measurement of the highest temperature fluids at each of the vent sites for trying to obtain the end-member pH values. This objective was greatly aided by the presence of a series of Ti-sheathed thermocouples immediately adjacent to the pH sensor. These thermocouples provided real time temperature data, while the sensor was being positioned in the vent fluid. Temperature maxima were achieved when the tip of the sensor was placed on top of the orifice or in contact with the inside wall of the chimney approximately up to 2–3 cm beneath the orifice (Fig. 1). In the case of flange pools associated with chimney structures at the Main Endeavour Field (MEF), the highest temperatures were encountered when the sensor was inserted as deeply as possible into the pooled fluid with the tip held against the underside of the flange [13]. The second deployment strategy was designed to trace changes in pH during cooling and mixing of the end-member hydrothermal fluid with seawater. This was accomplished by gradually moving the sensor tip from the interior to exterior of the fluid issuing from the vent orifice.

Real-time temperature and pH data (mV) for end-member hydrothermal vent fluid issuing from Dante vent (MEF) indicate amazing stability and also demonstrate a fast response of the sensor towards the fluid (Fig. 2). At Dante, stability is largely achieved by the existence of a quiescent pool of hot hydrothermal

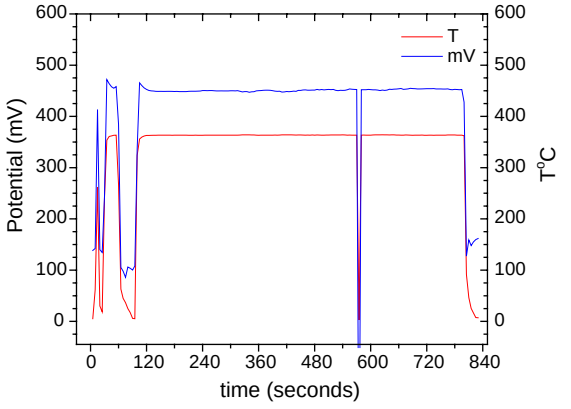

Fig. 2. A major advantage of the sensor design is that it allows simultaneous determination temperature and pH in a real time. Temperature data for fluid issuing from Dante vent (MEF) are depicted here by the trace in red, while emf (mV) data for $pH_{(in\ situ)}$ are shown by the blue trace. Data are taken every 5 s. The Fig. shows the response of the sensor to temperature and pH change. By positioning the sensor into the flange pool, stable chemical (pH) and thermal response is achieved, although a sudden infusion of cold seawater (~2 °C) at the 560 s interval resulted in a sharp drop in both temperature and mV output. Immediately following this, however, the signals returned to the previously established steady state condition.

fluid beneath a chimney flange structure that effectively minimizes mixing with seawater.

In general, vent fluids with the highest measured temperatures have the highest $pH_{(in\ situ)}$ values. For example, P-vent fluid (9°50′N EPR) and Dante and Hulk vent fluid (MEF, JDF) have temperatures and $pH_{(in\ situ)}$ of 384, 362 and 337 °C, and 5.4, 5.3 and 4.35, respectively (Fig. 3). Stability of the measured temperature, and the collection of fluids with near zero Mg concentration from these vents, indicate little, if any mixing with seawater, and provide the clearest indication yet of the pH of end-member vent fluid at mid-ocean ridges. Although no other in situ approach exists to corroborate these findings, they are generally consistent with results from a wide range of experimental and theoretical studies [3,5,6], which have long indicated that pH values in the vicinity of 5 are most consistent with phase equilibria constraints at conditions likely for vent fluid source regions. To illustrate this further for the specific vent fluid samples for which we have data, pH values were calculated at elevated pressures and temperatures ($pH_{(P,T)}$) using the measured pH ($pH_{25\ °C}$), while taking account of the distribution of aqueous species for which thermodynamic data are available [19–24] at the measured temperature and 250 bars (Table 1), the pressure at the seafloor at EPR 9°N, where the highest temperatures vent fluids are observed.

The difference between pH calculated ($pH_{(P,T)}$) and that actually measured in situ ($pH_{(in\ situ)}$) tends to be in the range of 0.1–0.4 units (Fig. 3). Although the agreement is especially good for vent fluids at Dante and Hulk, the offset is greater for P-vent fluids. This may be due to a combination of factors including uncertainties in available thermodynamic data, together with the lack of thermodynamic data for aqueous species in P-vent fluids at the requisite temperature and pressure conditions where the omission of such species may be particularly critical to pH calculation. Moreover, slight variations in temperature between fluid samples and pH-sensor measurements also likely contribute to variability between predicted and measured pH data, especially considering the sensitivity of thermodynamic data to temperature at conditions approaching the two phase boundary of seawater [19]. In sharp contrast with the relatively high $pH_{(in\ situ)}$ values, $pH_{(25\ °C)}$ does not exceed 4.0 for any of the end-member fluids (Fig. 3).

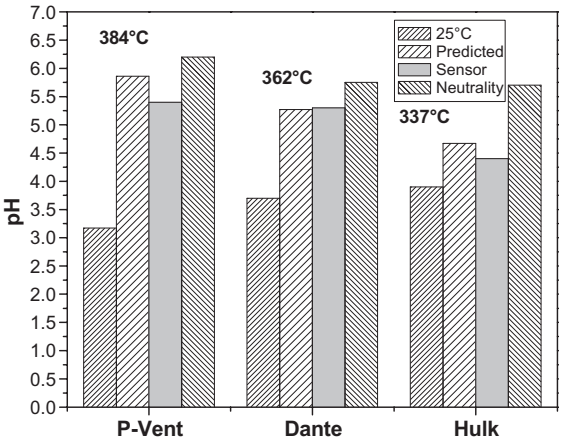

Fig. 3. $pH_{(in\ situ)}$ (measured) in comparison with that calculated for selected vent fluids from the MEF (Hulk, Dante) and EPR 9°50′N (P-vent) (see Table 1). $pH_{(in\ situ)}$ values increase with increasing temperature, but remain considerably more acid than neutrality at all conditions investigated. Dissociation of H^+-bearing aqueous species and mineralization effects combine to render $pH_{25\ °C}$ highly acidic. When these effects are accounted for using available thermodynamic data at appropriate *P–T* conditions, taking explicit account of vent fluid chemistry, however, agreement between pH predicted at elevated temperatures and pressures and measured in situ is generally within ±0.2–0.4 units (see text).

Table 1
Selected end member vent fluid chemistry used for calculating $pH_{(in\ situ)}$ (see Fig. 3)

Location	Dive no.	T °C	pH (25 °C)	Cl	Na	H_2S	K	Ca	Fe	Mn
P-vent*	3752	386	3.21	530	453	5.64	17.7	21.8	7.250	1.285
P-vent*	3764	385	3.13	531	464	6.40	17.5	21.7	7.396	1.279
Dante[27]	3470	350	3.72	418	333	13.0	22.8	27.5	2.00	0.475
Hulk[27]	3468	347	3.90	426	352	7.4	24.6	33.0	0.90	0.30

Units: mmol/kg, *K. L.Von Damm, unpublished data. Note: P-vent is located at EPR 9°50′N [28], while vents at Dante and Hulk are at the Main Endeavour Field, Northern Juan de Fuca Ridge [26,27]. Temperature differences between similar vents here and shown in Figs. 2 and 3 represent inherent variability at the time of sampling.

This is largely a result of the previously described dissociation of H^+-bearing aqueous complexes with cooling during sample processing [7,13,20]. Although pH of the high temperature end-member vent fluids may appear elevated, these values are still acidic, as indicted by comparison with the pH at neutrality at appropriate temperatures and pressures (Fig. 3) [23,24]. Thus, the measured $pH_{(in\ situ)}$ values of the end-member vent fluids from the Juan de Fuca Ridge and EPR 9°N provide the first direct confirmation of the long held inference of the weakly acidic character of hydrothermal fluids at elevated temperatures and pressures [29].

In addition to constraining pH of end-member vent fluids, sensor data can also be used to assess seawater-hydrothermal fluid mixing — a process that is of fundamental importance to mineralization, heat and mass transfer [30], as well as the existence of pH-sensitive microbial communities inhabiting seafloor chimney structures and underlying mounds. By incrementally moving the pH-sensor from the vent orifice through the interface between hydrothermal and seawater dominated environments, insight on pH controlling reactions associated with the compositional and thermal evolution of the vent fluid is obtained. For example, plotting $pH_{(in\ situ)}$ measurements against temperature reveals a "U-shaped" pattern (Fig. 4). Comparing the pH-temperature trend to neutrality at corresponding temperatures shows that mixing and cooling increase fluid acidity, especially at intermediate temperatures (250–300 °C). Theoretical calculations indicate that pH minima cannot be achieved by dissociation of H^+-bearing aqueous species alone, but rather require additional sources of acidity. One such source likely involves precipitation of pyrite and pyrrhotite from vent fluid derived dissolved Fe and H_2S, which give rise to the "blacksmoke" and ultimately chimney formation so characteristic of seafloor vents [2]. Although modest amounts of seawater mixing with vent fluid encourages precipitation of these phases [2], dilution and oxidation effects associated with greater seawater mixing ultimately limit mineral

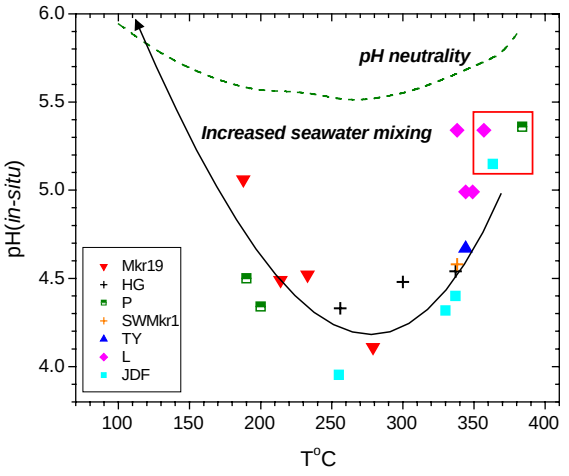

Fig. 4. $pH_{(in\ situ)}$ plotted against temperature for vent fluids from a wide range of axial locations. All cross symbols represent measurements from 21°N East Pacific Rise; data from the Main Endeavour Field (JDF) are shown as solid squares, while all the other symbols indicate data from 9°–10°N East Pacific Rise. The MEF data, however, specifically refer to vent fluids at Bastille, Hulk, and Dante sites. Other individual vent sites are as indicated in the Fig. legend. If more than one data point is plotted for a given site that with the higher temperature is more closely associated with the centre of the vent orifice. The data-enclosed box at relatively high-temperatures shows previously predicted pH values for end-member fluids investigated as part of the study. The "U-shaped" pattern exhibited when $pH_{(in\ situ)}$ is plotted against temperature results from seawater mixing as suggested by theoretical modelling studies [2,13]. Limited mixing effects cause dissociation of H^+-bearing complexes and metal sulphide precipitation, increasing fluid acidity. Greater degrees of mixing, result in seawater-dominated conditions with attendant pH increase (arrow trajectory).

precipitation, resulting in seawater dominated conditions and relatively high pH, as observed. On the other hand, conductive cooling of vent fluids acidified by mineralization effects within chimney walls could produce unusually acidic environments [31] and a likely ecosystem for acidophilic microbial communities, as have been recognized in subareal and hydrothermal deposits [32].

Data reported here demonstrate a powerful new technology that can be used to measure and monitor pH and dissolved gases in hydrothermal vent fluids. Considering the likely importance of pH and redox species as indicators of subseafloor alteration processes, seafloor mineralization, seawater mixing and biogeochemical processes, the new solid state sensors offer great promise for the eventual development of seafloor observatories designed in part to assess the chemical, biologic and physical evolution of hydrothermal vents systems at mid-ocean ridges and other submarine hydrothermal environments.

Acknowledgements

We thank Naibin Dong (UMN) and Ying Chen (ZJU) for assistance in development of the electronics package used with the pH sensor; Jeff Seewald (WHOI) and Michael E. Berndt (UMN) for assisting with acquisition of vent fluid chemistry during our 1999 cruise to the Main Endeavour Field (JDF). We also greatly acknowledge the pilots, officers and crewmembers of Atlantis/Alvin for their dedication and expertise, without which this study would not have been possible. The constructive reviews and suggestions provided by G. J. Massoth and I-Min Chou were particularly helpful and greatly appreciated. This work was supported by US National Science Foundation grants EAR-9614427 (K.D. and W.E.S.); OCE-9633132 (W.E.S., K.D. and M.K.T.); OCE-0117117 (W.E.S. and K.D.); OCE-9521436 and OCE-9633627 (M.K.T. and A.M.B.); and OCE-0002458 (K.L.V.D).

References

[1] J.M. Edmond, C. Measures, R.E. McDuff, L. Chan, R. Collier, B. Grant, L.I. Gordon, J. Corliss, Ridge crest hydrothermal activity and the balances of the major and minor elements in the ocean: the Galapagos data, Earth Planet. Sci. Lett. 46 (1979) 19–30.

[2] D.R. Janecky, W.E. Seyfried Jr., Formation of massive sulphide deposits on oceanic ridge crests: incremental reaction models for mixing between hydrothermal solutions and seawater, Geochim. Cosmochim. 48 (1984) 2723–2738.

[3] T.S. Bowers, H.P. Taylor Jr., An integrated chemical and stable-isotope model of the origin of mid-ocean ridge hot spring systems, J. Geophys. Res. 90 (1986) 12583–12606.

[4] T.S. Bowers, A.C. Campbell, C.I. Measures, A.J. Spivack, J.M. Edmond, Chemical controls on the composition of vent fluids at 13–11°N and 21°N East Pacific Rise, J. Geophys. Res. 93 (1988) 4522–4536.

[5] A.C. Campbell, M.R. Palmer, G.P. Klinkhammer, T.S. Bowers, J.M. Edmond, J.R. Lawrence, J.F. Casey, G. Thompson, S. Humphris, P. Rona, J.A. Karson, Chemistry of hot springs on the Mid-Atlantic Ridge, Nature 335 (1988) 514–519.

[6] W.E. Seyfried Jr., K. Ding, M.E. Berndt, Phase equilibria constraints on the chemistry of hot spring fluids at mid-ocean ridges, Geochim. Cosmochim. Acta 55 (1991) 3559–3580.

[7] K. Ding, W.E. Seyfried Jr., Determination of Fe–Cl complexing in the low pressure supercritical region (NaCl fluid)–Iron solubility constraints on pH of subseafloor hydrothermal fluids, Geochim. Cosmochim. Acta 56 (1992) 3681–3692.

[8] M.K. Tivey, Modeling chimney growth and associated fluid flow at seafloor hydrothermal vent sites, in: S.E. Humphris, R.A. Zierenberg, L.S. Mullineaux, R.E. Thomson (Eds.), Seafloor Hydrothermal Systems: Physical, Chemical, Biological, and Geochemical Interactions, American Geophysical Union, Washington, DC, 1995, pp. 158–177.

[9] H.C. Helgson, D.H. Kirkham, G.C. Flowers, Theoretical prediction of the thermodynamic behaviour of aqueous electrolytes at high pressures and temperatures: IV. Calculation of activity coefficients, osmotic coefficients, and apparent molal and standard and relative partial molal properties to 600 °C and 5 kb, Am. J. Sci. 281 (1981) 1249–1516.

[10] J.L. Bischoff, R.J. Rosenbauer, The critical point and two-phase boundary of seawater, 200–500 °C, Earth Planet. Sci. Lett. 68 (1984) 172–189.

[11] D.D. Macdonald, S. Hettiarachchi, H. Song, K. Makela, R. Emerson, M. Ben-Haim, Measurement of pH in subcritical and supercritical aqueous solutions, J. Solution Chem. 21 (1992) 849–881.

[12] K. Ding, W.E. Seyfied Jr., Direct pH measurement of NaCl-bearing fluid with an in situ sensor at 400 °C and 40 megapascals, Science 272 (1996) 1634–1636.

[13] K. Ding, W.E. Seyfried Jr., M.K. Tivey, A.M. Bradley, In situ measurement of dissolved H_2 and H_2S in high-temperature hydrothermal vent fluids at the Main Endeavour Field, Juan de Fuca Ridge, Earth Planet. Science Lett. 186 (2001) 417–425.

[14] T.J. Wolery, S.A. Daveler, EQ6, A Computer Program for Reaction Path Modeling of Aqueous Geochemical Systems: Theoretical Manual, Users Guide, and Related Documentation (version 7.0), 1992 (UCRL-MA-110662 PT IV, DOE, 1992).

[15] P.C. Ho, D.A. Palmer, M.S. Gruszkiewicz, Conductivity measurements of dilute aqueous HCl solutions to high temperatures and pressures using a flow-through cell, J. Phys. Chem. 105 (2001) 1260–1266.
[16] P.C. Ho, D.A. Palmer, R.E. Mesmer, Electrical conductivity measurements of aqueous sodium chloride solutions to 600 °C and 300 MPa, J. Solution Chem. 23 (1994) 997–1018.
[17] P.C. Ho, D.A. Palmer, R.H. Wood, Conductivity measurements of dilute aqueous LiOH, NaOH, and KOH solutions to high temperatures and pressures using a flow-through cell, J. Phys. Chem. 104 (2000) 12084–12089.
[18] P.C. Ho, H. Bianchi, D.A. Palmer, R.H. Wood, Conductivity of dilute aqueous electrolyte solutions at high temperatures and pressures using a flow cell, J. Solution Chem. 29 (2000) 217–235.
[19] J.L. Bischoff, R.J. Rosenbauer, Liquid-vapor relations in the critical region of the system NaCl–H_2O from 380 to 415 degree C: a refined determination of the critical point and two-phase boundary of seawater, Geochim. Cosmochim. Acta 52 (1988) 2121–2126.
[20] E.L. Shock, H.C. Helgeson, D.A. Sverjensky, Calculations of the thermodynamic and transport properties of aqueous species at high pressures and temperatures: standard partial molal properties of inorganic neutral species, Geochim. Cosmochim. Acta 53 (1989) 2157–2183.
[21] E.L. Shock, H.C. Helgeson, Calculations of the thermodynamic and transport properties of aqueous species at high pressures and temperatures: correlation algorithms for ionic species and equation of state predictions to 5 kb and 1000 °C, Geochim. Cosmochim. Acta 52 (1988) 2009–2036.
[22] A. Sverjensky, E.L. Shock, H.C. Helgeson, Prediction of the thermodynamic properties of aqueous metal complexes to 1000 °C and 5 kb, Geochim. Cosmochim. Acta 61 (1997) 1359–1412.
[23] J.W. Johnson, E.H. Oelkers, H.C. Helgeson, SUPCRT92-A software package for calculating the standard molal thermodynamic properties of minerals, gases, aqueous species, and reactions from 1-bar to 5000-bar and 0 °C to 1000 °C, Comput. Geosci. 18 (1992) 899–947.
[24] E.L. Shock, E.H. Oelkers, J.W. Johnson, D.A. Sverjensky, H.C. Helgeson, Calculation of the thermodynamic and transport properties of aqueous species at high pressures and temperatures: effective electrostatic radii to 1000 °C and 5 kb, J. Chem. Soc. Faraday Trans. 88 (1992) 803–826.
[25] A.M. Bradley, M.K. Tivey, S.P. Liberatore, A.R. Duester, Development and testing of thermocouple/thermistor array packages for monitoring temperature at hydrothermal vent sites, EOS Trans. Am. Geophys. Union 71 (1995) 411.
[26] W.E. Seyfried Jr., J.S. Seewald, M.E. Berndt, K. Ding, D. Foustoukos, Chemistry of hydrothermal vent fluids from the Main Endeavour Field, northern Juan de Fuca Ridge: geochemical controls in the aftermath of June 1999 seismic events, J. Geophys. Res. 108 (2003) 2429–2452.
[27] R.E. Butterfield, R.E. McDuff, M.J. Mottl, M.D. Lilley, J.E. Lupton, G.J. Massoth, Gradients in the composition of hydrothermal fluids from the Endeavor segment vent field: phase separation and brine loss, J. Geophys. Res. 99 (1994) 9561–9583.
[28] K.L. Von Damm, Controls on the chemistry and temporal variability of seafloor hydrothermal fluids, in: S.E. Humphris, R.A. Zierenberg, L.S. Mullineaux, R.E. Thomson (Eds.), Seafloor Hydrothermal Systems: Physical, Chemical, Biological, and Geochemical Interactions, American Geophysical Union, Washington, DC, 1995, pp. 222–247.
[29] H.L. Barnes, Solubilities of ore minerals, in: H.L. Barnes (Ed.), Geochemistry of Hydrothermal Ore Deposits, Wiley, New York, 1979, pp. 404–460.
[30] E.T. Baker, G.J. Massoth, C.E.J. de Ronde, J.E. Lupton, B.I. McInnes, Observations and sampling of an ongoing subsurface eruption of Kavachi volcano, Solomon islands, May 2000, Geology 30 (2002) 975–978.
[31] M.K. Tivey, The influence of hydrothermal fluid composition and advection rates on vent deposit mineralogy and texture: insights from modeling non-reactive transport, Geochim. Cosmochim. Acta 59 (1995) 1933–1949.
[32] S. Simmons, R. Norris, Acidophiles of saline water at vests of volcano, Extremophiles 6 (2002) 201–207.